ERJ open research
THE BEST IN OPEN ACCESS BASIC, TRANSLATIONAL & CLINICAL RESPIRATORY RESEARCH

Early View

Original research article

# Endobronchial optical coherence tomography or computed tomography for evaluating progression of bronchiectasis

Chang-hao Zhong, Chong-yang Duan, Zhu-quan Su

Please cite this article as: Zhong C-hao, Duan C-yang, Su Z-quan. Endobronchial optical coherence tomography or computed tomography for evaluating progression of bronchiectasis. *ERJ Open Res* 2023; in press (https://doi.org/10.1183/23120541.00490-2022).

## Original article

# Endobronchial optical coherence tomography or computed tomography for evaluating progression of bronchiectasis

**Lin-ling Cheng #1, M.D., Wei-jie Guan #1,2, Ph.D., Chang-hao Zhong 1, M.Med., Chong-yang Duan 3, Ph.D., Zhu-quan Su 1, Ph.D., Shi-yue Li *1, M.D., Nan-shan Zhong *1., M.D.**

1. State Key Laboratory of Respiratory Disease, National Clinical Research Center for Respiratory Disease, Guangzhou Institute of Respiratory Health, The First Affiliated Hospital of Guangzhou Medical University, Guangzhou Medical University, Guangzhou, China

2. Department of Thoracic Surgery, Guangzhou Institute of Respiratory Disease, The First Affiliated Hospital of Guangzhou Medical University, Guangzhou, Guangdong, China

3. State Key Laboratory of Organ Failure Research, National Clinical Research Center for Kidney Disease, Department of Biostatistics, School of Public Health, Southern Medical University, Guangzhou, China

**# Prof. Lin-ling Cheng and Wei-jie Guan are co-first authors**

*** Prof. Shi-yue Li and Nan-shan Zhong contributed equally to the work.**

**Main text**: 3915 words; **Abstract:** 250 words

***Corresponding author:** Nan-Shan Zhong. State Key Laboratory of Respiratory Disease, National Clinical Research Center for Respiratory Disease, Guangzhou Institute of Respiratory Health, The First Affiliated Hospital of Guangzhou Medical University, 151 Yanjiang Road, Guangzhou, Guangdong, China. Tel.: +86-20-83062729; Fax: +86-20-83062729; E-mail: nanshan@vip.163.com

**[Abstract]**

**Background:** The early radiologic signs of progression in bronchiectasis remain unclear.

**Objectives:** To compare endobronchial optical coherence tomography (EB-OCT) and chest computed tomography (CT) for evaluating radiological progression of bronchiectasis via stratifyng the presence (TW+) or absence (TW-) of thickened-walled bronchioles surrounding dilated bronchi among patients

with bronchiectasis based on CT, and determine the risk factors.

**Methods:** In this prospective cohort study, we performed both chest CT and EB-OCT at baseline and 5-year follow-up, to compare changes in airway caliber metrics. We evaluated bacterial microbiology, sputum matrix metalloproteinase-9 levels and free neutrophil elastase activity at baseline. We compared clinical characteristics and airway caliber metrics between group TW+ and TW-. We ascertained radiological progression at 5 years via CT and EB-OCT.

**Results:** We recruited 75 patients between 2014 and 2017. At baseline, EB-OCT metrics - mean luminal diameter ($P$=0.017), inner airway area ($P$=0.005), and airway wall area ($P$=0.009) of $7^{th}$-$9^{th}$ generation bronchioles were significantly greater in group TW+ than in group TW-. Meanwhile, EB-OCT did not reveal bronchiole dilatation (compared with the same segment of normal bronchioles) surrounding non-dilated bronchi on CT in group TW-. At 5 years, 53.1% of patients in group TW+ progressed to have bronchiectasis measured with EB-OCT, compared with only 3.3% in group TW- ($P$<0.05). 34 patients in group TW+ demonstrated marked dilatation of medium-sized and small airways. Higher baseline neutrophil elastase activity and TW+ bronchioles on CT predicted progression of bronchiectasis.

**Conclusion:** Thickened-walled bronchioles surrounding the dilated bronchi, identified with EB-OCT, indicates progression of bronchiectasis.

**[Key words]** Early Bronchiectasis; Prognosis; High-resolution Computed Tomography; Endobronchial Optical Coherence Tomography

**Competing interest:** None declared.

**Funding/support:** National Natural Science Foundation No. 82170003 (to Prof Cheng), The Study of the Common Key Technologies of Large-scale Development of Novel Inhaled Preparations No. 2017ZX09201002 (National Science and Technology Major Project of the Ministry of Science and Technology of China) (to Prof. Zhong), National Natural Science Foundation - Outstanding Youth Fund (No. N82222001), National Natural Science Foundation No. 81870003, Guangdong Science and Technology Foundation (No. 2019B030316028), Zhongnanshan Medical Foundation of Guangdong

Province No. ZNSA-2020013 and Guangzhou Science and Technology Plans (No. 2023B03J0407 and No. 202102010372), Plan on enhancing scientific research in Guangzhou Medical University (to Prof. Guan).

**Author contributions:** L. L. C., W. J. G., C. H. Z., Z. Q. S., S. Y. L. and N. S. Z. were responsible for patient recruitment and collected individual data; C. Y. D. performed statistical analyses; L. L. C., S. Y. L. and N. S. Z. contributed to study conception; L. L. C. and W. J. G. drafted the manuscript; S. Y. L. and N. S. Z. provided critical review of the manuscript and approved the final submission.

**E-mail address:**

**Lin-ling Cheng,** linling@gird.cn

**Wei-Jie Guan,** battery203@163.com

**Chang-hao Zhong,** vast1982@126.com

**Chong-yang Duan**, donyduang@126.com

**Zhu-quan Su,** py1011xiaoquan@163.com

**Shi-yue Li,** lishiyue@188.com

**Nan-Shan Zhong,** nanshan@vip.163.com

**Take-home messages**

EB-OCT imaging could reveal the evolution of thickened-walled bronchioles surrounding the dilated bronchi, indicating radiologic progression of bronchiectasis.

## Introduction

Bronchiectasis is pathologically defined as the irreversible dilation of the tracheobronchial tree. Because chronic airway infections, inflammation and destruction have been the core elements driving the progression of bronchiectasis [1], breaking this vicious cycle is central to the treatment of bronchiectasis. Early identification and diagnosis may help improve the management of bronchiectasis [2,3].

Few studies, however, have revealed the mechanisms of pathogenesis, especially how bronchiectasis initially develops [4,5]. Chest high-resolution computed tomography (HRCT) images have revealed that the bronchioles with thickened walls surrounding the dilated bronchi might progress into the typical radiologic bronchiectasis [6,7]. However, without the use of sophisticated and quantitative analytic softwares that have not been extensively adopted for clinical application, chest HRCT might be capable of evaluating the airways up to the sixth generation bronchi. Direct airway morphological assessment may help to probe the early morphological changes (bronchial dilatation and remodeling) with a greater resolution. The advent of endobronchial optical coherence tomography (EB-OCT) [8,9,10] has made it possible to evaluate the structural changes (including airway wall thickening) up to the ninth generation of bronchi in a real-time fashion.

We performed a longitudinal study with EB-OCT and chest CT to determine their diagnostic value for evaluating radiolocal progression of bronchiectasis via stratifyng patients according to the presence/absence of tree-in-bud signs (the frequent chest imaging characteristics indicative of bronchial wall thickening) surrounding the dilated bronchi on chest HRCT images to the typical radiologic bronchiectasis, and to explore the risk factors. Our findings may provide the rationale for early intervention of the bronchial dilatation with inflammatory infiltration to prevent from the progression to clinically significant bronchiectasis.

## Methods

### *Study population*

Between July 2014 and February 2017, we recruited consecutive patients with symptomatic bronchiectasis (part of the *Progressive Bronchiectasis Early Surveillance Program*) from Guangzhou Institute of Respiratory Diseases. Eligible patients had radiologic evidence of bronchiectasis, as evaluated centrally with chest HRCT by an experienced radiologist [11]. Patients were dichotomized

into two groups based on the presence or absence of radiologist-reported tree-in-bud signs on baseline HRCT: 1) those with tree-in-bud signs surrounding dilated bronchi (Group TW+), and 2) those without tree-in-bud signs surrounding dilated bronchi (Group TW-). All patients underwent OCT, HRCT, spirometry and sputum induction on the same day at baseline and 5-year longitudinal follow-up (no interim reassessments were performed). At longitudinal follow-up, the radiological progression of bronchiectasis was ascertained via both EB-OCT and HRCT.

The disease control group consisted of nine patients who underwent bronchoscopy for biopsy of lung nodules within the study time frame. Patients in the disease control group underwent a single chest HRCT and EB-OCT assessment at the initial visit only (no follow-up visits).

The study was approved by the ethics committee of the First Affiliated Hospital of Guangzhou Medical University (Medical Ethics Approval 2014 [No. 51]), and all patients provided written informed consent.

***Chest HRCT, Spirometry, and Bronchiectasis Severity Index assessment***

Unenhanced chest CT examinations were performed using different commercial CT scanners at baseline (Aquilion 16, Toshiba, Japan) and follow-up visits (Perspective 64, Seimens, Germany). Images were acquired during breath-hold at full inspiration. The fixed tube voltage was 120 kVp with adaptive current modulation. The raw imaging data were reconstructed into 2 mm slice thickness with the soft-tissue algorithm at baseline and 1 mm slice thickness at follow-up, respectively. The three-dimensional bronchial tree images were reconstructed using the Direct Path navigation system (version 1.1, Olympus, Osaka, Japan). Bronchiectasis was diagnosed if the internal diameter of bronchi was greater than that of the accompanying pulmonary artery, a lack of normal bronchial tapering, or visible bronchi within 10 mm of the pleural surface. Tree-in-bud sign referred to the centrilobular bronchial dilatation filled with mucus, pus, or fluid [7]. The radiologic severity of bronchiectasis was scaled by using a modified Reiff score on a lobar basis, where the lingular lobe was regarded as a separate lobe [12]. The maximal total score was 18 for six lobes [13]. Radiologic progression of bronchiectasis was defined as the evolvement from the initial tree-in-bud sign or thickened bronchial walls into the typical signs of bronchiectasis. Two chest radiologists (with 16 and 23 years experience) independently scored the chest CT images. Progression of bronchiectasis could be ascertained only when the two radiologists reached a consensus.

Spirometry was conducted by using spirometers (QUARK PFT, COSMED Inc., Milan, Italy),

complying with the American Thoracic Society/European Respiratory Society guidelines [14]. Variation between the best two maneuvers was <5% or 200ml in forced vital capacity and forced expiratory volume in one second ($FEV_1$), with the maximal values being reported. The predicted values were calculated according to the model proposed by Zheng et al [15].

Bronchiectasis Severity Index (BSI) [16] was adopted to rate the severity of bronchiectasis. The BSI comprised the age, body-mass index, prior exacerbations and prior hospitalization in the preceding year, $FEV_1$ predicted%, Medical Research Council dyspnea score, the number of bronchiectatic lobes, *Pseudomonas aeruginosa* infection, and colonization with other PPMs. The BSI of ≤4, 5-8 and ≥9 denoted mild, moderate and severe bronchiectasis, respectively.

***Navigation planning, EB-OCT Data Acquisition and Analysis***

To more accurately evaluate airway structural changes (particularly the small airways), we performed EB-OCT assessment of the 3$^{rd}$ to 9$^{th}$ generation bronchi surrounding the radiologically dilated bronchi. For patients in group TW+, we initially labeled for EB-OCT measurement with the Direct Path version 1.1 navigation system (Olympus, Osaka, Japan), and advanced the detector to the bronchi with thickened walls or bud-in-tree sign surrounding the radiologically dilated bronchi on chest HRCT images. Typically, we selected 3-5 regions of interest (ROI) where there were tree-in-bud signs within the diameter of 2 cm of the dilated bronchi on chest CT. The entry of these ROIs into the CT navigation system would allow us to establish a pathway which stemmed from the large airways to the tree-in-bud signs (bronchioles). We selected the ROIs within the diameter of 2 cm of the dilated bronchi on CT images because most of these affected bronchioles have already been located in the 9$^{th}$ generation bronchi (the detection limit of EB-OCT) or more distal bronchioles. Only the ninth generation of the right lung bronchus 9 segment was subject to EB-OCT assessment among disease controls. In our study, around 87% of patiens in group TW- were subject to the measurement of the airway caliber at the same lung lobe as compared with those in group TW+. The 9$^{th}$ generation bronchi of the right lower lobe were evaluated as the control airway segment in a minority of patients who did not have bronchiectasis in the same lung lobe.

The bronchoscope with an EB-OCT detector was advanced into the target lobe with the Lightlabs C7XR OCT system (St. Jude Medical). The probe's outer diameter was 0.9 mm (C7 Dragonfly catheters), which could automatically rotate and pull back. We inserted the scanning probe with an ultrafine flexible bronchoscope (B260f; Olympus; outer diameter: 2.8 mm, internal diameter: 1.2 mm)

to the labeled target bronchus, according to the planned pathway generated by the DirectPath system. Patients held their breath after full inspiration. The EB-OCT catheter was pulled back to the third-generation bronchus for automatic scanning. The identical virtual path was established for each patient to guide the EB-OCT detector for advancing to an identical anatomical location. The EB-OCT scan was performed at a rotary frame rate of 180Hz and a pullback rate of 1.8 cm/s, and hence 540 consecutive EB-OCT images were generated in each pullback procedure (length: 5.4cm) within 3 seconds. EB-OCT parameters included the mean luminal diameter (Dmean), inner airway area (Ai) and airway wall area (Aw) from the third to ninth generation. The airway wall area percentage (Aw%) was calculated as [Aw/(Ai + Aw)]×100% [17]. The EB-OCT parameters detected from the 3$^{rd}$ to 4$^{th}$, from the 5$^{th}$ to 6$^{th}$, and from the 7$^{th}$ to 9$^{th}$ generation of bronchi were averaged, respectively, to reflect the morphology of the large, medium-sized and small airways. Data were analyzed using a computerized software (OCT system software, St. Jude Medical). The normal range of the airway caliber has been published previously [8].

***Sputum induction***

Fresh induced sputum was sampled via induction with hypertonic saline (3%~5%) during hospital visits. Following removal of contents in oral cavity and chest physical therapy for 15 minutes, patients expectorated into 60ml sterile clear plastic container. Eligible samples should have 25 leukocytes or greater and 10 epithelial cells or lower under microscopic field (×100). Within 2 hours, sputum was split for bacterial culture and ultracentrifugation (50,000g) at 4℃ for 90 minutes to prepare for sputum sol stored in -80℃ freezers until further measurements.

***Sputum bacterial culture***

The methods for sputum bacterial culture have been described previously [13]. Briefly, fresh sputum was homogenized, followed by inoculation for overnight culture. Potentially pathogenic microorganisms (PPMs) consisted of *Pseudomonas aeruginosa* (PA), *Haemophilus influenzae*, *Haemophilus parainfluenzae* and miscellaneous clinically significant bacteria [18]. Bacterial load, expressed as the colony forming unit per milliliter (cfu/ml), was reported for the PPMs only.

***Sputum biomarker assessments***

Sputum matrix metalloproteinase-9 (MMP-9) level was measured by using Luminex multiplex assay (Biorad Inc., USA) [13] with the Bioplex reader (Biorad Inc., USA). The lower and upper bound of detection was (0.14, 302.50) ng/ml for MMP-9. Free neutrophil elastase (NE) activity was quantified

in sputum supernatant by using an NE activity assay kit according to the manufacturer`s instructions (Cayman Chemicals, Ann Arbor, MI, USA). Measurements were performed in duplicates and the mean was included for further analysis.

***Statistical analysis***

No formal sample size calculation could be made due to the lack of existing morphological data. We empirically aimed to recruit more than 50 patients each in the group TW+ and TW-. Currently, the gold standard for defining the upper limit of the normal absolute internal diameter of bronchi is lacking. We defined bronchiectasis according to EB-OCT provided that the airway internal diameter measured with EB-OCT at baseline was two times greater than that of the same corresponding bronchial segment among the age-matched healthy controls [8].

For the between-group comparisons, numerical data were presented as mean ± standard deviation for normal distribution or otherwise as median (interquartile range), and were compared by using the two-sample independent t-test or Wilcoxon rank-sum test. Categorical data were expressed as the number (percentage) and compared with chi-square test. Bonferroni correction was applied to adjust for multiple comparisons. Correlation analyses were conducted by using Pearson's or Spearman's model, with or without adjustment for confounding factors (age, sex, body-mass index). We calculated the difference of EB-OCT parameters by subtracting the values of the 5-year reassessment with that of the baseline levels.

Univariable logistic regression model was used to determine the associations between the radiologic progression of bronchiectasis on EB-OCT and the clinical variables, including age, female sex, body-mass index, smoking status, the duration of disease, respiratory symptoms at baseline, modified Reiff score, bronchiectasis severity index (BSI), exacerbations within the previous 2 years, forced expiratory volume in one second ($FEV_1$) predicted%, TW+, sputum NE activity and MMP-9 levels at baseline, sputum bacterial density at baseline, and the detection of PA at baseline. We only included the parameters with both the statistical ($P \leq 0.10$) and clinical significance into the multivariable logistic regression model: the BSI, exacerbations within the previous 2 years, $FEV_1$ predicted%, TW+, sputum NE activity and MMP-9 levels at baseline, and the detection of PA at baseline.

Statistical analysis was performed using SPSS, version 16.0 (SPSS Inc., USA) and GraphPad Prism 5.0 (GraphPad Inc., USA). $P<0.05$ was deemed statistically significant for all analyses unless

otherwise stated.

Patients or the public were not involved in the design, or conduct, or reporting, or dissemination plans of our research.

## Results

### *Patient characteristics*

Of 137 patients with bronchiectasis who underwent screening at baseline, 69 with tree-in-bud signs surrounding the dilated bronchi (TW+) and 68 patients without tree-in-bud signs surrounding the dilated bronchi (TW-) were included. Sixty-two patients were excluded due to a variety of reasons (e.g., consent withdrawal or lost to follow-up), 75 patients and 9 disease controls were included in the final analysis (**Figure 1**).

**Table 1** presents the baseline demographics and clinical characteristics. The BSI was comparable between group TW+ and group TW- ($P>0.05$). A higher proportion of patients in group TW+ had post-infectious bronchiectasis and isolation of PA than in group TW- (both $P<0.05$). Compared with group TW-, group TW+ had a lower BMI and more severe airflow limitation (both $P<0.05$). Most patients (98.4% in group TW+ and 96.7% in group TW-) had used mucolytics within 6 months, followed by theophylline (73.4% in group TW+ and 68.9% in group TW-).

### *Bronchiectasis detected with EB-OCT and HRCT measurement at the baseline visit*

For the $7^{th}$ to $9^{th}$ generation of bronchi at baseline, the baseline EB-OCT metrics $D_{mean}$ (mean: 3.96 vs 2.05 mm, $P$=0.017), Ai (mean: 10.25 vs 4.27 $mm^2$, $P$=0.005), Aw (mean: 2.61 vs 0.83 $mm^2$, $P$=0.009) and Aw% (mean: 19.64% vs 17.85%, $P$=0.039) of the bronchioles with thickened walls surrounding the dilated bronchioles (TW+) on CT images were significantly greater than those of the same bronchiole segments in group TW-. However, at the $3^{rd}$-$6^{th}$ generation of bronchi, there were no significant differences in the $D_{mean}$, Ai and Aw between group TW+ and group TW- at baseline visit (all $P>0.05$) (**Table 2**). The tree-in-bud signs were mainly located in the lower lobes (67.2%), followed by the middle (including the lingula) lobe (28.1%).

### *Progression of bronchiectasis detected with EB-OCT and HRCT measurement*

For the $5^{th}$-$6^{th}$ generation bronchi, there was a significant increase from baseline in $D_{mean}$ (mean difference: 2.17, 95%CI: 1.04, 4.29), Ai (mean difference: 14.39, 95%CI: 8.63, 21.64) and Aw (mean difference: 2.68, 95%CI: 2.12, 3.06) and a decrease in the Aw% (mean difference: -3.1, 95%CI: -5.21,

-1.37) at 5-year follow-up in group TW+, but not in group TW-. For the $7^{th}$ -$9^{th}$ generation bronchi, we also noted a significant increase from baseline in the $D_{mean}$ (mean difference: 1.97, 95%CI: 1.59, 2.75), Ai (mean difference: 17.66, 95%CI: 9.54, 21.84) and Aw (mean difference: 2.67, 95%CI: 1.48, 3.94) and a decrease in the Aw% (mean difference: -3.27, 95%CI: -6.16, -1.72) at 5-year follow-up in group TW+, but not in group TW- (**Table 2**).

At 5-year follow-up, the proportion of patients with an increase from baseline in the magnitude of bronchiectasis, measured with EB-OCT, was markedly higher in group TW+ than in group TW- (53.1% vs. 3.3%, $P$<0.05). Of the 64 patients in group TW+, 15 had developed typical bronchiectasis (11 cases in the lower lobes, 8 cases in the middle lobe and 4 cases in both the middle and lower lobes). Meanwhile, the magnitude of bronchiectasis in HRCT scan was greater in group TW+ than in group TW- (23.4% vs. 0%, $P$<0.05) as compared with baseline (**Figure 1**). Furthermore, the bronchioles with radiologically visible thickened walls on the initial CT scans developed into the typical columnar or cystic bronchiectasis on HRCT at 5 years (**Figure 2**).

***Longitudinal EB-OCT measurement of the bronchioles***

To confirm the structural changes of bronchioles on HRCT images obtained with EB-OCT, we next labeled the $7^{th}$ to $9^{th}$ generation of bronchi surrounding the dilated bronchi in the navigation system, which corresponded to the tree-in-bud signs of the same segment shown on chest HRCT (**Figure 3**). We also compared the changes during longitudinal follow-up with EB-OCT measurement. **Figure 4** demonstrates the representative cross-sectional EB-OCT images of the $3^{rd}$, $5^{th}$, $7^{th}$ and $9^{th}$ generation of bronchi in a 52-year-old female patient in group TW+ at baseline and at 5 years, and in a 46-year-old male patient with lung cancer (in TW- group) at baseline.

At 5 years, 34 out of 64 bronchiectasis patients in group TW+ (53.1%) demonstrated a marked dilatation of both the medium-sized (from the $5^{rd}$ to $6^{th}$ generation) and small airways (from the $7^{th}$ to $9^{th}$ generation). However, no marked dilatation was observed corresponding to the $3^{rd}$ and $4^{th}$ generation bronchi at 5 years. There was a notable increase in the $D_{5-6}$ (mean: 3.90 vs 6.07 mm, $P$<0.05), $Ai_{5-6}$ (mean: 13.76 vs 28.15 $mm^2$, $P$<0.05), $D_{7-9}$ (mean: 3.96 vs 5.93 mm, $P$<0.05) and $Ai_{7-9}$ (mean: 10.25 vs 27.91 $mm^2$, $P$<0.05) at 5 years as compared with the baseline levels (**Table 2**). At 5 years, there were no significant changes in the EB-OCT metrics of all airway segments (large-to-medium plus small airways) in group TW- [$D_{3-4}$ (mean: 5.21 vs 4.88 mm, $P$>0.05), $Ai_{3-4}$ (mean: 24.61 vs 21.75 $mm^2$, $P$>0.05); $D_{5-6}$ (mean: 3.84 vs 4.20 mm, $P$>0.05), $Ai_{5-6}$ (mean: 17.18 vs 19.50 $mm^2$,

*P*>0.05); $D_{7\text{-}9}$ (mean: 2.05 vs 2.28 mm, *P*>0.05) and $Ai_{7\text{-}9}$ (mean: 4.27 vs 4.64 $mm^2$, *P*>0.05)] compared with the baseline levels. According to the assessment made by two indepdenent radiologists, there were no significant changes in the airway diameter (progression to radiologically typical bronchiectasis) on chest HRCT in group TW-.

***Associations between the progression on EB-OCT assessment and clinical characteristics of bronchiectasis***

The associations between the progression of bronchiectasis measured with EB-OCT and the clinical characteristics (e.g., CT parameters, lung function, inflammatory markers and microbiology) are shown in **Table 3**. Multivariable logistic regression analysis was performed to determine the factors associated with the EB-OCT progression of bronchiectasis. Higher sputum NE activity (OR=1.05, 95%CI: 1.01~1.10, *P*=0.030) and the TW+ bronchioles on chest CT images (OR=140.42, 95%CI: 1.03~19077.11, *P*=0.048) were independently associated with the progression of bronchiectasis on EB-OCT.

## Discussion

Progression of bronchiectasis has been attributed to the vicious cycle of chronic airway infection, inflammation and destruction [1]. Few studies have explored the morphological and the radiologic progression of bronchiectatic airways based on the cohort study designs. How the unaffected bronchi progressed into the radiologically typical bronchiectasis remains unclear. In this study, we have demonstrated the longitudinal changes in the morphological characteristics of the dilated bronchi, evidenced by the thickened wall bronchioles surrounding the dilated bronchi visible on chest HRCT, or the tree-in-bud signs detected with EB-OCT. Our findings have provided the higher-resolution images of different airway segments (particularly the small airways) in a real-time fashion. Apart from the higher sputum NE activity, the presence of bronchioles with thickened walls surrounding the dilated bronchi on HRCT at baseline could independently predict the progression of bronchiectasis at 5 years of follow-up.

Because of the limited resolution of chest HRCT, we have characterized the small airways with EB-OCT, which has been used to evaluate small airways in patients with COPD [17]. Identifying the events that predated the development of typical bronchiectasis may provide further clues to inform

clinicians the key signs of radiologic bronchiectasis progression. The vicious vortex hypothesis posits that both airway infection and inflammation (also indicated by the mucus plugging or infiltration) are imperative drivers of bronchiectasis. To this end, we have specifically focused on the TW+ bronchi which are mainly localized in the small airways. In our study, the EB-OCT criteria detected more patients with radiological progression of bronchiectasis than the HRCT criteria could be partly interpreted by the greater ability of EB-OCT to directly evaluate the morphology of more distal airways. The difficulty in identifying the subtle structural changes in small airways could be circumvented with EB-OCT assessment. Here, we showed that the radiological bronchiectasis was more pronounced in small airways (mostly at the $7^{th}$ to $9^{th}$ generation bronchi) which had significant bronchial wall thickening and luminal dilatation, compared with the same bronchiolar segments from the disease controls. However, neither the increased wall thickness of the proximal ($3^{rd}$ to $5^{th}$ generation) bronchi nor the dilatation of the bronchial lumen was not evident (**Figure 3, Table 2**). This might be because the distal bronchial wall thickness was less notable than that of the proximal bronchial wall, thus appearing more susceptible to the insult of the inflammatory responses or enzymatic digestion [19]. Due to the limited resolution, early-stage bronchial dilatation (particularly at the distal airways) could not be readily distinguished in the HRCT apart from the tree-in-bud signs or bronchi with thickened walls [20].

Not all bronchi with tree-in-bud signs or thickened walls would develop into typical radiologic bronchiectasis. A previous study has reported that bronchiectasis was more prominent in the bronchioles surrounding the dilated bronchi [21]. Therefore, the lesion with dilatation of the bronchioles surrounding the radiologically typical dilated bronchi might be regarded as the characteristic sign of bronchiectasis. To verify this finding, we have performed EB-OCT assessment on the bronchioles in patients with interstitial pneumonia and bronchiolitis obliterans with tree-in-bud signs or bronchiolitis on chest HRCT in our pilot study, with findings showing that these patients had thickening of the bronchial wall without bronchiectasis on both chest HRCT and EB-OCT images (Cheng LL, et al. unpublished data). Therefore, the bronchioles with thickened walls surrounding the bronchi are susceptible of progression into the typical radiologic dilatation. The diagnosis of these early signs of bronchiectasis could be based on the specific HRCT imaging characteristics (such as tree-in-bud signs or bronchi with thickened walls surrounding the dilated bronchi). EB-OCT might be valuable for detecting the *early-stage* bronchiectasis (**Figure 1, Figure 3**). Our findings have

provided the evidence that distal bronchiole dilation and higher sputum bacterial loads, higher concentration of sputum MMP-8 and -9 might be predictors of the development of typical bronchiectasis on HRCT [22,23]. Our findings have also lent support to the previous observation that higher NE activity was the key predictor of bronchiectasis development in children with cystic fibrosis [24].

Progression to bronchiectasis has been observed in a subgroup of patients with cystic fibrosis [25]. In a study which recruited 168 patients with cystic fibrosis who had no detectable bronchiectasis on the first chest CT scan, 94 patients (56%) developed into radiologically typical bronchiectasis within one year [25]. Furthermore, air trapping on chest HRCT was associated with the subsequent development of typical bronchiectasis. Our findings indicated that progressive bronchial dilatation might have occurred in the bronchioles with thickened walls which cannot be detected on the initial HRCT. The air trapping might be related to the thickening of the bronchial wall as well as mucus hypersecretion that resulted in mucus plugging and dynamic hyperinflation.

Notably, the bronchial dilatation surrounding the radiologically visible dilated bronchi independently predicted the development of typical bronchiectasis (**Table 3**). Our findings have added to the vicious cycle theory that the progression of bronchiectasis could have resulted from the aggravated airway infections, heightened inflammatory responses and persistent airway destruction [26]. In line with our observations, Mott et al. also found that the radiological progression of bronchiectasis was associated with heightened neutrophilic inflammation [25]. Furthermore, the heightened elastase activity in sputum was associated with the bronchiectasis severity index and radiological extent of bronchiectasis [27].

Some limitations should be taken into account. The detection of the more distal airways (e.g., the $10^{th}$ generation and beyond) remains challenging because the EB-OCT detector could not reach beyond the $9^{th}$ generation, which has hampered the imaging of smaller or more distal bronchi surrounding the dilated bronchus shown on the chest CT. Moreover, because of the airway structural changes (e.g., alveolar or bronchiolar damage), the precise localization of same the bronchioles before and after the 5-year longitudinal follow-up might not be feasible in some of the patients despite the use of the automated computerized software. Therefore, our data could not confirm whether the typical bronchiectasis evolved from the same dilated airway with early signs of bronchiectasis. Follow-up studies with a longer duration would enable a better longitudinal comparisons of the airway structural

changes, thus providing greater insights into the patterns of bronchiectasis progression.

In summary, EB-OCT assessment reveals that the wall thickening of airways surrounding the dilated bronchi independently predicts the progression into radiologically typical bronchiectasis. Our findings have further lent support to the vicious vortex hypothesis, suggesting the need of early detection and intervention of bronchiectasis to halt the vicious cycle.

**Abbreviations**

HRCT: high-resolution computed tomography

EB-OCT: endobronchial optical coherence tomography

TW+: tree-in-bud signs (bronchial wall thickening) surrounding the dilated bronchi

TW-: no tree-in-bud signs surrounding the dilated bronchi

Dmean: mean luminal diameter

Ai: inner airway area

Aw: airway wall area

Aw%: airway wall area percentage

PPMs: potentially pathogenic microorganisms

PA: *Pseudomonas aeruginosa*

cfu/ml: colony forming unit per milliliter

MMP-9: matrix metalloproteinase-9

NE: neutrophil elastase

BSI: bronchiectasis severity index

$FEV_1$: forced expiratory volume in one second

## References

1. McShane PJ, Naureckas ET, Tino G, Strek ME. Non-cystic fibrosis bronchiectasis. *Am J Respir Crit Care Med* 2013; 188: 647-656.

2. Barker AF. Bronchiectasis. *N Engl J Med* 2002; 346: 1383-1393.

3. Li AM, Sonnappa S, Lex C, Wong E, Zacharasiewicz A, Bush A, Jaffe A. Non-CF bronchiectasis: does knowing the aetiology lead to changes in management? *Eur Respir J* 2005; 26: 8-14.

4. Tepper LA, Caudri D, Rovira AP, Tiddens HA, de Bruijne M. The development of bronchiectasis on chest computed tomography in children with cystic fibrosis: can pre-stages be identified? *Eur Radiol* 2016; 26: 4563-4569.

5. Flume PA, Chalmers JD, Olivier KN. Advances in bronchiectasis: endotyping, genetics, microbiome, and disease heterogeneity. *Lancet* 2018; 392: 880-890.

6. Guan WJ, Gao YH, Xu G, Lin ZY, Tang Y, Li HM, Lin ZM, Zheng JP, Chen RC, Zhong NS. Characterization of lung function impairment in adults with bronchiectasis. *PLoS One* 2014; 9: e113373.

7. Gosset N, Bankier AA, Eisenberg RL. Tree-in-bud pattern. *Am J Roentgenol* 2009; 193: W472-477.

8. Su ZQ, Guan WJ, Li SY, Feng JX, Zhou ZQ, Chen Y, Zhong ML, Zhong NS. Evaluation of the Normal Airway Morphology Using Optical Coherence Tomography. *Chest* 2019; 156: 915-925.

9. Hou R, Le T, Murgu SD, Chen Z, Brenner M. Recent advances in optical coherence tomography for the diagnoses of lung disorders. *Expert Rev Respir Med* 2011; 5: 711-724.

10. Chen Y, Ding M, Guan WJ, Wang W, Luo WZ, Zhong CH, Jiang M, Jiang JH, Gu YY, Li SY, Zhong NS. Validation of human small airway measurements using endobronchial optical coherence tomography. *Respir Med* 2015; 109: 1446-1453.

11. Feldman C. Bronchiectasis: new approaches to diagnosis and management. Clin Chest Med 2011; 32: 535-546.

12. Pasteur MC, Helliwell SM, Houghton SJ, Webb SC, Foweraker JE, Coulden RA, Flower CD, Bilton D, Keogan MT. An investigation into causative factors in patients with bronchiectasis. *Am J Respir Crit Care Med* 2000; 162: 1277-1284.

13. Guan WJ, Gao YH, Xu G, Lin ZY, Tang Y, Gu YY, Liu GH, Li HM, Chen RC, Zhong NS. Sputum matrix metalloproteinase-8 and -9 and tissue inhibitor of metalloproteinase-1 in bronchiectasis: clinical correlates and prognostic implications. *Respirology* 2015; 20: 1073-1081.

14. Laszio G. ATS/ERS task force: Standardization of spirometry. *Eur Respir J* 2005; 26: 319–338.

15. Zheng JP, Zhong NS. Normative values of pulmonary function testing in Chinese adults. *Chin Med J* 2002; 115: 50-54.

16. Chalmers JD, Goeminne P, Aliberti S, McDonnell MJ, Lonni S, Davidson J, Poppelwell L, Salih

W, Pesci A, Dupont LJ, Fardon TC, De Soyza A, Hill AT. The bronchiectasis severity index: An international derivation and validation study. *Am J Respir Crit Care Med* 2014; 189: 576-85.

17. Ding M, Chen Y, Guan WJ, Zhong CH, Jiang M, Luo WZ, Chen XB, Tang CL, Tang Y, Jian QM, Wang W, Li SY, Zhong NS. Measuring Airway Remodeling in Patients With Different COPD Staging Using Endobronchial Optical Coherence Tomography. *Chest* 2016; 150: 1281-1290.

18. Tunney MM, Einarsson GG, Wei L, Drain M, Klem ER, Cardwell C, Ennis M, Boucher RC, Wolfgang MC, Elborn JS. Lung microbiota and bacterial abundance in patients with bronchiectasis when clinically stable and during exacerbation. *Am J Respir Crit Care Med* 2013; 187: 1118-1126.

19. Marini T, Hobbs SK, Chaturvedi A, Kaproth-Joslin K. Beyond bronchitis: a review of the congenital and acquired abnormalities of the bronchus. *Ins Imag* 2017; 8: 141-153.

20. Hansell DM. Small airways diseases: detection and insights with computed tomography. *Eur Respir J* 2001; 17: 1294-1313.

21. Milliron B, Henry TS, Veeraraghavan S, Little BP. Bronchiectasis: Mechanisms and Imaging Clues of Associated Common and Uncommon Diseases. *Radiographics* 2015; 35: 1011-1030.

22. Pasteur MC, Bilton D, Hill AT. British Thoracic Society guideline for non-CF bronchiectasis. *Thorax* 2010; 65 Suppl 1: i1-58.

23. Wang D, Luo J, Du W, Zhang LL, He LX, Liu CT. A morphologic study of the airway structure abnormalities in patients with asthma by high-resolution computed tomography. *J Thorac Dis* 2016; 8: 2697-2708.

24. Sly PD, Gangell CL, Chen L, Ware RS, Ranganathan S, Mott LS, Murray CP, Stick SM; AREST CF. Risk factors for bronchiectasis in children with cystic fibrosis. *N Engl J Med* 2013; 368: 1963-70.

25. Mott LS, Park J, Murray CP, Gangell CL, de Klerk NH, Robinson PJ, Robertson CF, Ranganathan SC, Sly PD, Stick SM. Progression of early structural lung disease in young children with cystic fibrosis assessed using CT. *Thorax* 2012; 67: 509-516.

26. Guan WJ, Gao YH, Xu G, Li HM, Yuan JJ, Zheng JP, Chen RC, Zhong NS. Bronchodilator response in adults with bronchiectasis: correlation with clinical parameters and prognostic implications. *J Thorac Dis* 2016; 8: 14-23.

27. Chalmers JD, Moffitt KL, Suarez-Cuartin G, Sibila O, Finch S, Furrie E, Dicker A, Wrobel K, Elborn JS, Walker B, Martin SL, Marshall SE, Huang JT, Fardon TC. Neutrophil Elastase Activity Is Associated with Exacerbations and Lung Function Decline in Bronchiectasis. *Am J Respir Crit Care*

*Med* 2017; 195: 1384-1393.

**Figure legends**

**Figure 1. Subject recruitment flowchart**

**Figure 2. longitudinal changes in chest radiologic manifestations in a patient in group TW+ and a patient in group TW- during the 5-year follow-up.**

A1-A2: longitudinal changes in chest radiologic manifestations in a 77-year-old male (group TW+); B1-B2: longitudinal changes in chest radiologic manifestations in a 49-year-old male (group TW-). The bronchioles surrounding the dilated bronchi are characterized by thickened walls or tree-in-bud signs but no significant dilatation is shown on chest high-resolution computed tomographic scans at the initial visit (A1). There are markedly dilated bronchioles at the same bronchial segment within the same patient after 5 years of follow-up (A2). However, no tree-in-bud signs are developed after years of follow-up in a patient who does not have tree-in-bud signs at the initial visit (B1 and B2).

**Figure 3. Chest high-resolution computed tomographic scans and the visualization with an automated navigation system**

Chest HRCT images were obtained at 0.5-1.0 mm collimation in DICOM format, and transformed into the DirectPath version 1.1 navigation system (Olympus, Japan) for reconstruction of three-dimensional bronchial tree images. The bronchioles surrounding the dilated bronchi were labeled and the guided pathways were generated. The bronchoscope with detector was passed into the target bronchiole for EB-OCT measurement according to the planned pathway generated by DirectPath system.

Panels A1, B1, C1 and D1 display the cross-sectional images of the carina (A), right main bronchus (B), right upper lobe bronchus (C) and the target bronchiole (D) for the virtual path. Panel E demonstrates the simulated guidance pathway (blue curve) to the target bronchiole (entry of the fiber bronchoscopy probe from the trachea to the target bronchiole).

**Figure 4. Cross-sectional endobronchial optical coherence tomography images of multiple airway generations in patients with (TW+) and without (TW-) tree-in-bud signs on CT**

Cross-sectional images of endobronchial optical coherence tomography in the (A) $3^{rd}$, (B) $5^{th}$, (C) $7^{th}$, and (D) $9^{th}$ generation bronchi. A1, B1, C1 and D1 denotes EB-OCT images of the $3^{rd}$, $5^{th}$, $7^{th}$ and $9^{th}$ generation bronchi in group TW-. A2, B2, C2 and D2 denotes the EB-OCT images of the $3^{rd}$, $5^{th}$, $7^{th}$ and $9^{th}$ generation bronchi in group TW+ at baseline, and A3, B3, C3 and D3 denotes the EB-OCT

images of the 3rd, 5th, 7th and 9th generation bronchi in group TW+ at 5 years.

Compared with the images derived from the same bronchial segment of a representative patient in group TW- (C1, D1), the mean luminal diameter (Dmean), inner luminal area (Ai) and airway wall area (Aw) of the bronchioles with thickened walls surrounding the dilated bronchioles on CT images are significantly greater at the 7th to 9th generation of bronchi at the initial visit (C2, D2). Meanwhile, no differences could be found in the Dmean, Ai and Aw between the bronchioles at the 3rd to 5th generation between a representative patient in group TW+ (A1, B1) and group TW- (A2, B2). At 5 years, there has been a marked dilatation of the 5th as well as from the 7th to 9th generation of bronchi (B3, C3, D3) as compared with the tree-in-bud signs at baseline (B2, C2, D2). No marked dilatation of the 3rd generation bronchi was noted (A3).

The images at panels A2-D2 (at baseline) and A3-D3 (at 5-year longitudinal follow-up) were derived from the same bronchiectasis patient.

## Table 1. Baseline levels of the bronchiectasis patients

| Parameter | TW + (n=64) | TW - (n=61) | P |
|---|---|---|---|
| **Anthropometry** | | | |
| Age, years, mean ± SD | 53.6±16.6 | 54.8±17.0 | 0.684 |
| BMI, kg/m$^2$, median [IQR] | 19.34±2.21 | 20.29±3.44 | 0.039 |
| Females (No., %) | 39 (60.9) | 31 (50.8) | 0.238 |
| Non-smokers (No., %) | 51 (79.7) | 49 (80.3) | 0.929 |
| **Disease-related parameters** | | | |
| Disease duration, years, median [IQR] | 3.5 [2.3, 4.9] | 3.3 [2.1, 4.8] | 0.810 |
| Acute exacerbations within 2 years, median [IQR] | 2 [1, 2] | 2 [1, 2] | 0.213 |
| Bronchiectasis severity index, median [IQR] | 3 [2, 4] | 2 [2, 3] | 0.06 |
| **Imaging characteristics** | | | |
| No. of bronchiectatic lobes, median [IQR] | 3 [2, 3] | 2 [2, 3] | 0.153 |
| Modified Reiff score for HRCT, median [IQR] | 3.5 [3, 4] | 3 [2, 4] | 0.032 |
| No. of lung segments with tree-in-bud signs, median [IQR] | 1 [1, 2] | 0 [0, 0] | 0.00 |
| Location of tree-in-bud sign | | | |
| Upper lobe (No., %) | 3 (4.7) | 0 | 0.260 |
| Middle and lingula lobe (No., %) | 18 (28.1) | 0 | <0.001 |
| Lower lobe (No., %) | 43 (67.2) | 0 | <0.001 |
| **Lung function indices** | | | |
| $FEV_1$ predicted %, mean ± SD | 54.3±15.8 | 62±19.6 | 0.018 |
| FVC predicted %, mean ± SD | 68.3±11.3 | 78.1±19.2 | 0.001 |
| $FEV_1$/FVC%, mean ± SD | 68.4±14.4 | 70.7±14.1 | 0.359 |
| $DL_{CO}$ predicted %, mean ± SD | 74.3±19.4 | 86.4±17.4 | <0.001 |
| **Aetiology** | | | |
| Post-infectious (No., %) | 24 (37.5) | 13 (21.3) | 0.047 |
| Immunodeficiency (No., %) | 9 (14.1) | 7 (11.5) | 0.665 |
| Miscellaneous (No., %) | 5 (7.8) | 8 (13.1) | 0.332 |
| Idiopathic (No., %) | 26 (40.6) | 33 (54.1) | 0.131 |
| **Sputum bacteriology** | | | |
| *Pseudomonas aeruginosa* (No., %) | 48 (75) | 6 (9.8) | <0.001 |
| *Haemophilus influenzae* (No., %) | 6 (9.4) | 17 (27.9) | 0.008 |
| Other potentially pathogenic bacteria (No., %) | 1 (1.6) | 11 (18) | 0.002 |
| Commensals (No., %) | 1 (1.6) | 13 (21.3) | <0.001 |
| **Medications ever used within 6 months** | | | |
| Inhaled corticosteroids (No., %) | 7 (10.9) | 6 (9.8) | 0.840 |
| Mucolytics (No., %) | 63 (98.4) | 59 (96.7) | 0.531 |
| Theophylline (No., %) | 47 (73.4) | 42 (68.9) | 0.571 |
| Macrolides (No., %) | 23 (35.9) | 26 (42.6) | 0.444 |

## Table 2. EB-OCT Parameters at baseline and 5 years

| | | | Group TW+ | | | | Group TW- | | | | | |
|---|---|---|---|---|---|---|---|---|---|---|---|---|
| | **EB-OCT Parameters** | **Control** | **Baseline (n=64)** | **5 years (n=39)** | **Difference * (95%CI)** | **P Value** | **Baseline (n=61)** | **5 years (n=36)** | **Difference * (95%CI)** | **P Value** | **$P^a$ Value** | **$P^b$ Value** |
| **Large airways** | **$D_{3-4}$ (mm)** | 5.60±1.08 | 5.05±1.96 | 5.23 ± 2.09 | 0.18 (-0.21, 1.16) | 0.388 | 5.21±2.08 | 4.88±1.38 | -0.33 (-1.13, 0.48) | 0.514 | 0.277 | 0.387 |
| | **$Ai_{3-4}$ ($mm^2$)** | 25.51±9.69 | 23.23±18.05 | 26.71 ± 12.48 | 3.48(-1.61, 10.37) | 0.074 | 24.61±17.97 | 21.75±9.69 | -2.86 (-9.85, 4.13) | 0.652 | 0.739 | 0.152 |
| | **$Aw_{3-4}$ ($mm^2$)** | 3.33±0.97 | 3.71±0.91 | 3.41 ± 1.46 | -0.30 (-0.94, 0.11) | 0.539 | 2.79±1.00 | 3.52±1.32 | 0.73 (0.17, 1.28) | 0.148 | 0.085 | 0.528 |
| **Medium-sized airways** | **$D_{5-6}$ (mm)** | 3.76±1.26 | 3.90±1.03 | 6.07 ± 2.39 | 2.17 (1.04, 4.29) | 0.011 | 3.84±0.90 | 4.20±1.10 | 0.49 (-0.03, 1.02) | 0.761 | 0.671 | 0.029 |
| | **$Ai_{5-6}$ ($mm^2$)** | 18.27±6.11 | 13.76±6.78 | 28.15 ± 4.31 | 14.39 (8.63, 21.64) | 0.006 | 17.18 ±8.27 | 19.50±8.46 | 2.46 (-2.17, 7.09) | 0.079 | 0.084 | 0.008 |
| | **$Aw_{5-6}$($mm^2$)** | 2.05 ±0.31 | 1.96±0.29 | 4.64 ± 0.82 | 2.68 (2.12, 3.06) | 0.015 | 1.95 ±0.28 | 2.27±0.39 | 0.35 (0.16, 0.54) | 0.236 | 0.373 | 0.013 |
| | **$Aw_{5-6}$%** | 11.20 ±4.59 | 16.66 ± 9.10 | 13.56 ± 5.81 | -3.1 (-5.21, -1.37) | 0.042 | 13.79±12.47 | 12.10±5.36 | -1.97 (-7.21, 3.26) | 0.442 | 0.086 | 0.041 |
| **Small airways** | **$D_{7-9}$ (mm)** | 1.84±0.46 | 3.96 ± 0.91 | 5.93 ± 1.54 | 1.97 (1.59, 2.75) | 0.029 | 2.05±0.63 | 2.28±0.51 | 0.22 (-0.10, 0.53) | 0.752 | 0.017 | 0.002 |
| | **$Ai_{7-9}$ ($mm^2$)** | 3.32 ±1.66 | 10.25±4.62 | 27.91 ± 4.73 | 17.66 (9.54, 21.84) | 0.004 | 4.27±2.05 | 4.64±2.38 | 0.43 (-0.81, 1.67) | 0.493 | 0.005 | 0.001 |
| | **$Aw_{7-9}$ ($mm^2$)** | 0.62 ±0.31 | 2.61 ± 0.84 | 5.28 ± 1.93 | 2.67 (1.48, 3.94) | 0.027 | 0.83±0.33 | 0.76 ±0.11 | -0.11 (-0.24, 0.03) | 0.516 | 0.009 | 0.001 |
| | **$Aw_{7-9}$%** | 16.70±5.25 | 19.64 ± 7.38 | 16.37 ± 3.87 | -3.27 (-6.16, -1.72) | 0.016 | 17.85±10.91 | 17.49±9.87 | -1.14 (-6.89, 4.62) | 0.691 | 0.039 | 0.027 |

* Shown are the values of the 5-year reassessment minus that of the baseline levels.

5-6 = from fifth- to sixth-generation bronchi; 7-9 = from seventh- to ninth-generation bronchi; Ai = inner luminal area; Aw = airway wall area; D = inner diameter; EB-OCT = endobronchial optical coherence tomography.

a = The P value for the comparison of each of the EB-OCT parameter between group TW+ and group TW- at baseline.

b = The P value for the comparison of each of the EB-OCT parameter between group TW+ and group TW- at 5 years.

TW+: The bronchioles with thickened walls around dilated bronchioles (tree-in-bud sign) on CT image

TW-: The bronchioles without thickened walls around dilated bronchioles (tree-in-bud sign) on CT image

## Table 3. Clinical factors associated with progression of bronchiectasis

| Clinical factors | Progression of bronchiectasis on EB-OCT | | Univariable model | | Multivariable model | |
|---|---|---|---|---|---|---|
| | No (n=39) | Yes (n=36) | OR (95% CI) | p Value | OR (95% CI) | p Value |
| Age | 56.5±16.7 | 50.4±17.6 | 0.98 [0.95~1.01] | 0.124 | - | - |
| Sex (female) | 19 (48.7%) | 23 (63.9%) | 0.54 [0.21~1.36] | 0.188 | - | - |
| BMI | 20.2±3.3 | 19.0±2.2 | 0.85 [0.72~1.01] | 0.064 | - | - |
| Non-smoker (%) | 32 (82.1%) | 27 (75%) | 1.52 [0.50~4.64] | 0.458 | - | - |
| Duration of bronchiectasis (years) | 3.5 [2.2~5.6] | 3.1 [2.3~4.7] | 0.88 [0.69~1.11] | 0.278 | - | - |
| Modified Reiff score for HRCT | 3.0 [2.0~4.0] | 4.0 [3.0~6.0] | 1.68 [1.20~2.36] | 0.003 | - | - |
| Bronchiectasis severity index (BSI) | 2.0 [2.0~3.0] | 4.0 [3.0~4.3] | 2.48 [1.52~4.04] | <0.001 | 2.08 [0.48~9.06] | 0.330 |
| Exacerbations within previous 2 years | 1.0 [1.0~2.0] | 2.0 [1.0~3.0] | 1.79 [1.10~2.92] | 0.020 | 1.10 [0.12~10.21] | 0.935 |
| FEV1 predicted % | 61.0[41.1~78.7] | 54.3 [42.0~67.3] | 0.98 [0.96~1.01] | 0.148 | 1.01 [0.92~1.11] | 0.850 |
| Respiratory symptoms at the initial visit | 28(71.8%) | 31 (86.1%) | 1.96 [0.64~6.02] | 0.237 | - | - |
| Sputum NE activity at the initial visit (μg/mL) | 37.3 [22.6~70.9] | 154.4 [123.8~173.4] | 1.06 [1.03~1.10] | 0.000 | 1.05 [1.01~1.10] | 0.030 |
| Sputum MMP-9 at the initial visit (ng/mL) | 353.3 [200.8~599.6] | 1790.0 [1382.1~2509.0] | 1.00 [1.00~1.01] | 0.000 | 1.00 [1.00~1.00] | 0.681 |
| PA at the initial visit | 2 (5.1%) | 31 (86.1%) | 5.13 [1.91~13.80] | 0.001 | 4.18 [0.27~65.50] | 0.308 |
| Sputum bacterial densities at the initial visit ($\times 10^7$ cfu/ml ) | 6.4 [6.0~7.2] | 7.1 [6.0~7.5] | 1.06 [0.76~1.49] | 0.724 | - | - |
| TW+ | 5 (12.8%) | 34 (94.4%) | 115.60 [20.96~637.45] | <0.001 | 140.42 [1.03~19077.11] | 0.048 |
| Inhaled corticosteroids | 4 (10.3%) | 4 (11.1%) | - | - | - | - |
| Macrolides | 17 (43.6%) | 10 (27.8%) | - | - | - | - |
| Mucolytics | 39 (100%) | 36 (100%) | - | - | - | - |
| Theophylline | 33 (84.6) | 26 (72.2%) | - | - | - | - |

Univariate logistic regression model was used to determine the associations between the radiologic progression of bronchiectasis on EB-OCT and the clinical variables, including age, female sex, body-mass index, smoking status, the duration of disease, respiratory symptoms at baseline, modified Reiff score, bronchiectasis severity index (BSI), exacerbations within the previous 2 years, forced expiratory volume in one second ($FEV_1$) predicted%, TW+, sputum NE activity and MMP-9 levels at baseline, sputum bacterial density at baseline, and the detection of PA at baseline.

We only included the parameters with both the statistical (*P* value of 0.10 or less) and clinical significance into the multivariate logistic regression model: the BSI, exacerbations within the previous 2 years, $FEV_1$ predicted%, TW+, sputum NE activity and MMP-9 levels at baseline, and the detection of PA at baseline.

TW+: The bronchioles with thickened walls around dilated bronchioles (tree-in-bud sign) on CT image

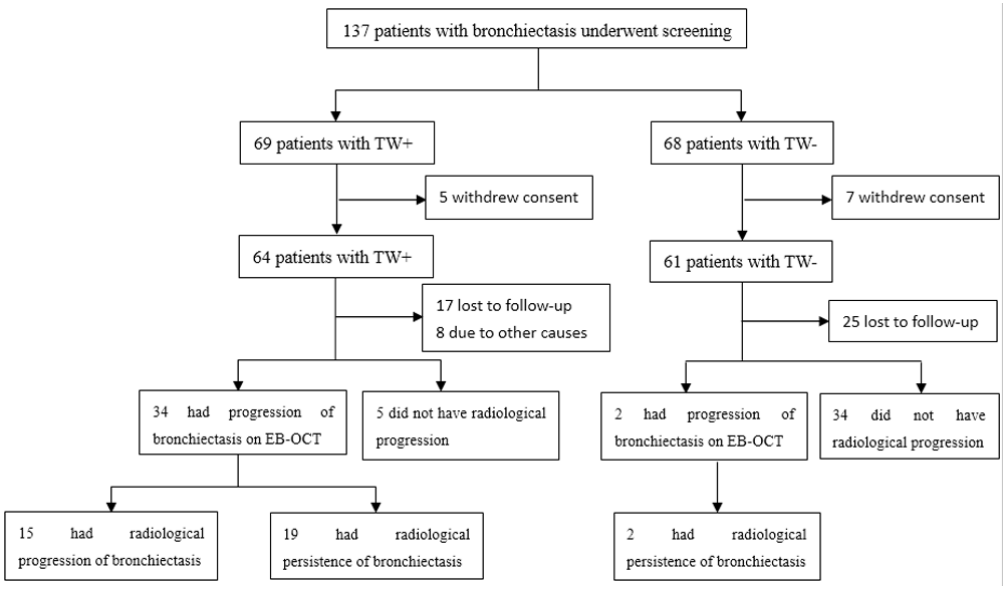


Figure 1. Subject recruitment flowchart

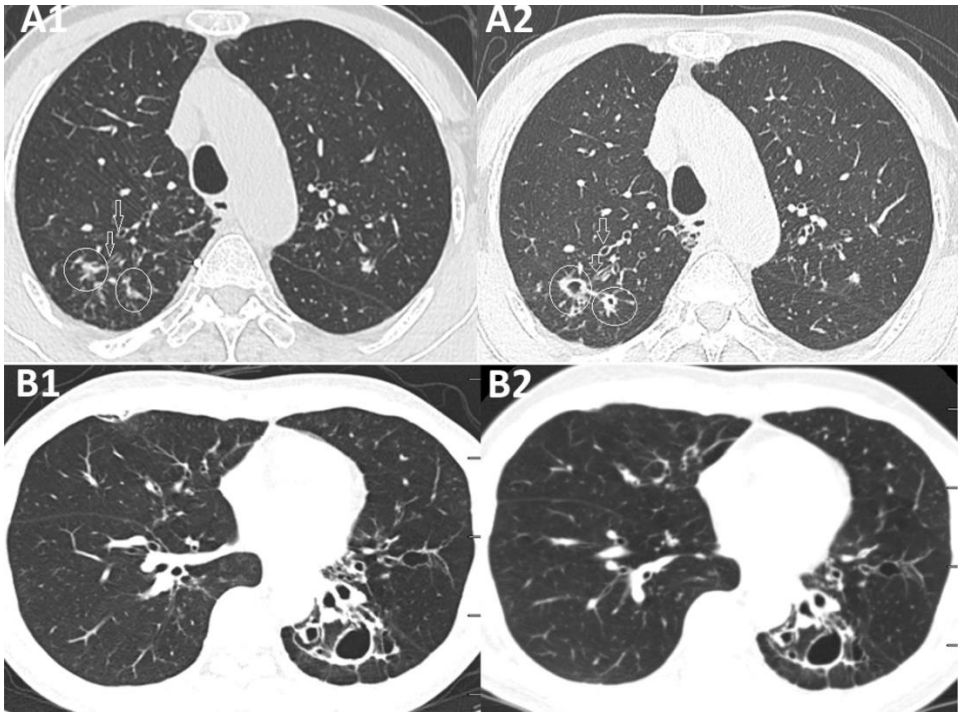


Figure 2. longitudinal changes in chest radiologic manifestations in a patient in group TW+ and a patient in group TW- during the 5-year follow-up. A1-A2: longitudinal changes in chest radiologic manifestations in a 77-year-old male (group TW+); B1-B2: longitudinal changes in chest radiologic manifestations in a 49-year-old male (group TW-). The bronchioles surrounding the dilated bronchi are characterized by thickened walls or tree-in-bud signs but no significant dilatation is shown on chest high-resolution computed tomographic scans at the initial visit (A1). There are markedly dilated bronchioles at the same bronchial segment within the same patient after 5 years of follow-up (A2). However, no tree-in-bud signs are developed after years of follow-up in a patient who does not have tree-in-bud signs at the initial visit (B1 and B2).

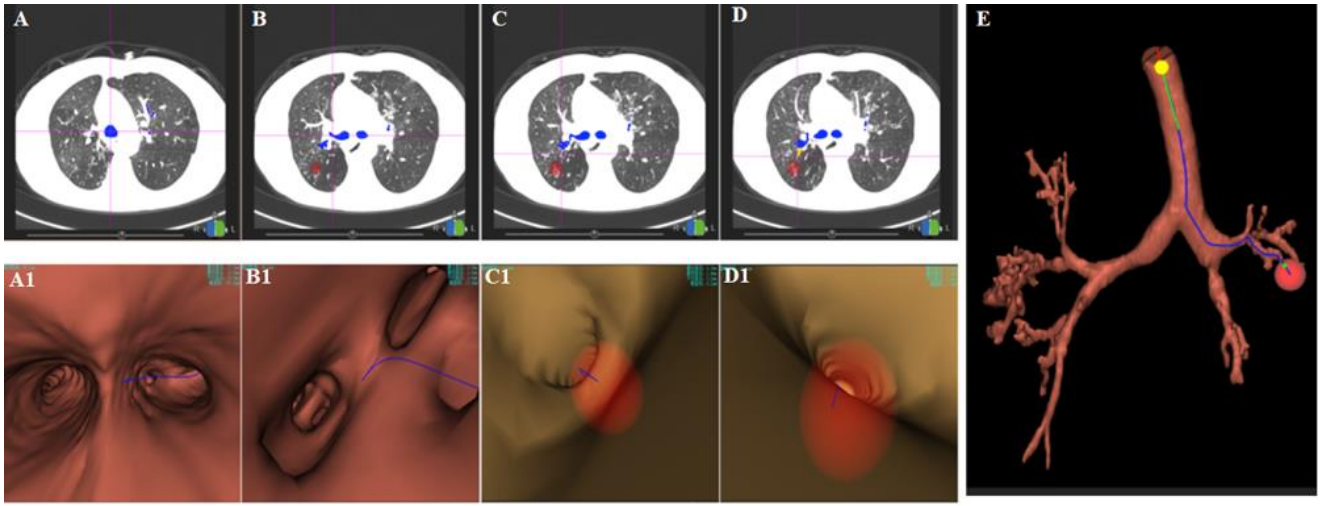


Figure 3. Chest high-resolution computed tomographic scans and the visualization with an automated navigation system Chest HRCT images were obtained at 0.5-1.0 mm collimation in DICOM format, and transformed into the DirectPath version 1.1 navigation system (Olympus, Japan) for reconstruction of three-dimensional bronchial tree images. The bronchioles surrounding the dilated bronchi were labeled and the guided pathways were generated. The bronchoscope with detector was passed into the target bronchiole for EB-OCT measurement according to the planned pathway generated by DirectPath system. Panels A1, B1, C1 and D1 display the cross-sectional images of the carina (A), right main bronchus (B), right upper lobe bronchus (C) and the target bronchiole (D) for the virtual path. Panel E demonstrates the simulated guidance pathway (blue curve) to the target bronchiole (entry of the fiber bronchoscopy probe from the trachea to the target bronchiole).

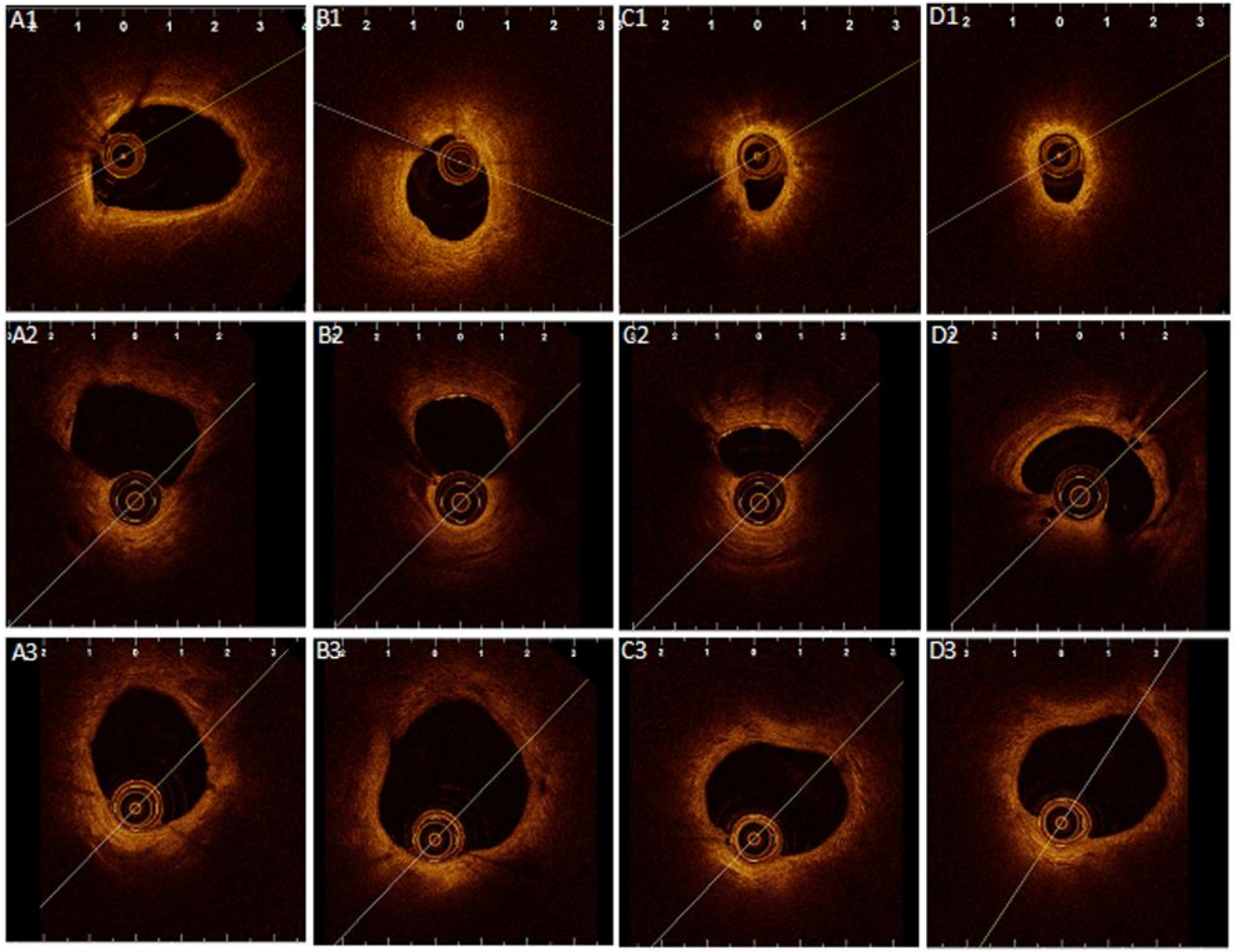


Figure 4. Cross-sectional endobronchial optical coherence tomography images of multiple airway generations in patients with (TW+) and without (TW-) tree-in-bud signs on CT Cross-sectional images of endobronchial optical coherence tomography in the (A) 3rd, (B) 5th, (C) 7th, and (D) 9th generation bronchi. A1, B1, C1 and D1 denotes EB-OCT images of the 3rd, 5th, 7th and 9$^{th}$ generation bronchi in group TW-. A2, B2, C2 and D2 denotes the EB-OCT images of the 3rd, 5th, 7th and 9th generation bronchi in group TW+ at enrollment, and A3, B3, C3 and D3 denotes the EB-OCT images of the 3rd, 5th, 7th

and 9th generation bronchi in group TW+ at 5 years. Compared with the images derived from the same bronchial segment of a representative patient in group TW- (C1, D1), the mean luminal diameter (Dmean), inner luminal area (Ai) and airway wall area (Aw) of the bronchioles with thickened walls surrounding the dilated bronchioles on CT images are significantly greater at the 7th to 9th generation of bronchi at the initial visit (C2, D2). Meanwhile, no differences could be found in the Dmean, Ai and Aw between the bronchioles at the 3rd to 5th generation between a representative patient in group TW+ (A1, B1) and group TW- (A2, B2). At 5 years, there has been a marked dilatation of the 5th as well as from the 7th to 9th generation of bronchi (B3, C3, D3) as compared with the tree-in-bud signs at enrollment (B2, C2, D2). No marked dilatation of the 3rd generation bronchi was noted (A3). The images at panels A2-D2 (at enrollment) and A3-D3 (at 5-year longitudinal follow-up) were derived from the same bronchiectasis patient.